Check for updates

Physics of Semiconductors. Semiconductors

UDC 661.691, 546.22/.24

EDN MBYUNH
https://www.doi.org/10.33910/2687-153X-2025-6-2-93-103

Thermal and laser crystallization of InSe thin films formed by vacuum thermal evaporation

M. E. Fedyanina ✉[1], V. B. Pestova [1, 2], D. V. Pepelyaev [1, 3], Ya. S. Lebedeva [1, 2], A. V. Babich [1], M. P. Smayev [1, 4], A. V. Romashkin [1], S. I. Nesterov [5], S. A. Kozyukhin [1, 3]

[1] National Research University of Electronic Technology, 1 Shokina Sq., Zelenograd 124498, Russia
[2] Herzen State Pedagogical University of Russia, 48 Moika Emb., Saint Petersburg 191186, Russia
[3] Kurnakov Institute of General and Inorganic Chemistry, 31 Leninsky Ave., Moscow 119991, Russia
[4] Lebedev Physical Institute of the Russian Academy of Sciences, 53 Leninsky Ave., Moscow 119991, Russia
[5] Ioffe Physical-Technical Institute, 26 Polytekhnicheskaya Str., Saint Petersburg 194021, Russia

Authors

Mariya E. Fedyanina, ORCID: 0000-0001-9779-2574, e-mail: mahamaha1996@gmail.com

Victoria B. Pestova, ORCID: 0000-0003-0781-0375, e-mail: kapakycek2009@yandex.ru

Dmitry V. Pepelyaev, ORCID: 0000-0002-9281-484X, e-mail: pepelyaev-dima@mail.ru

Yana S. Lebedeva, ORCID: 0000-0002-8128-1080, e-mail: generalova97@gmail.com

Alexey V. Babich, ORCID: 0000-0003-2999-8049, e-mail: drent@yandex.ru

Mikhail P. Smayev, ORCID: 0000-0003-1351-5209, e-mail: smayev@lebedev.ru

Alexey V. Romashkin, ORCID: 0000-0002-0101-6122, e-mail: romaleval@gmail.com

Sergey I. Nesterov, ORCID: 0000-0003-1166-9087, e-mail: nesterovru@mail.ru

Sergey A. Kozyukhin, ORCID: 0000-0002-7405-551X, e-mail: sergkoz@igic.ras.ru

For citation: Fedyanina, M. E., Pestova, V. B., Pepelyaev, D. V., Lebedeva, Ya. S., Babich, A. V., Smayev, M. P., Romashkin, A. V., Nesterov, S. I., Kozyukhin, S. A. (2025) Thermal and laser crystallization of InSe thin films formed by vacuum thermal evaporation. *Physics of Complex Systems*, 6 (2), 93–103. https://www.doi.org/10.33910/2687-153X-2025-6-2-93-103
EDN MBYUNH

Received 1 December 2024; reviewed 19 March 2025; accepted 19 March 2025.

Funding: Sample fabrication and experimental work were supported by the Russian Science Foundation (project No. 22-19-00766) with contributions from the Research Laboratory of Active Photonic Materials and Devices. Raman spectroscopy and AFM measurements were supported by the Ministry of Science and Higher Education of the Russian Federation in the framework of state task (FSMR-2023-0002).

Abstract. Binary chalcogenides have found a wide range of applications due to the possibility of fast and reversible phase transitions, tunable band gap, and high charge carrier mobility. This paper presents the results of thermal and laser crystallization of InSe thin films deposited by vacuum thermal evaporation of synthesized material and covered with a protective SiO_2 layer. The amorphous state of as-deposited InSe thin films was confirmed by Raman spectroscopy. Thermal and laser crystallization processes were studied using electrical resistivity measurements and optical microscopy respectively. The temperature and laser power ranges required for the crystallization of the InSe thin film were determined. The Raman spectroscopy showed that the degree of crystallinity of modified regions of InSe thin films can be tuned by varying the power of laser irradiation.

Keywords: chalcogenide materials, binary compounds, InSe, optical properties, structural properties, laser crystallization

Introduction

In recent decades, thin chalcogenide films have attracted considerable attention due to their unique electrical and optical properties, which make it possible to implement various devices for storing and processing data, and for the modulation and conversion of optical radiation. Of special interest is the control of the properties of materials through changing the phase state or van der Waals gap reconfiguration — for example, through the application of uniaxial compression (Stepanov 2024). Numerous applications of chalcogenide materials and greater attention to two-dimensional chalcogenide structures have fostered the study of $A^{III}B^{VI}$ system. It includes InSe, which is an n-type layered semiconductor with a band gap of 1.2–1.3 eV (Darwish et al. 2013; Kovalyuk et al. 2005). InSe structures with a small number of layers allow an adjustment of the optical band gap in the range of 1.4–2.6 eV and are characterized by an extremely high mobility of charge carriers (Bandurin et al. 2017).

Currently, the possibility of creating InSe-based photosensitive elements is widely discussed (Song et al. 2020). The formation of photodetectors with different architectures, including photodetectors with simultaneous use of 1D and 2D objects (Dai et al. 2018), has been described in previous studies (Feng et al. 2015; Wang et al. 2020). Besides, the use of InSe in flexible electronics (Zhao et al. 2019), optical fibers and for the implementation of photoinduced structural transformations (Xin et al. 2024) opens up significant prospects.

Featuring prominently among the main methods for obtaining InSe film samples are the electrodeposition technique (Gopal et al. 2004), molecular beam epitaxy (Emery et al. 1989; Voigt et al. 2024b), chemical vapor deposition (Chang et al. 2018; Park et al. 2003), and thermal evaporation (El-Nahass et al. 2012; Kobbi, Kesri 2004). Depending on the method, growth conditions, and parameters, InSe films can be also obtained as either amorphous or crystalline. In (Mustafa et al. 2010) In_xSe_{1-x} thin films were prepared using the thermal evaporation technique, while the XRD analysis confirmed the amorphous structure of the deposited films. This film formation method enables the study of the crystallization process, which, in phase-change materials, is a lower-temperature and longer process compared to amorphization.

Unlike other chalcogenide materials, such as materials of the Ge–Sb–Te system (Prikryl et al. 2022; Rybin et al. 2021; Smayev et al. 2024), Sb_2Se_3 (Lebedeva et al. 2023), or MoS_2 (Rani et al. 2017; Tran-Khac et al. 2019), phase transformation study by laser modification in InSe film samples has not produced many results so far. Laser irradiation with millisecond pulses of amorphous In_2Se_3 films prepared by thermal evaporation crystallizes thin film samples into a monoclinic phase (Khusayfan et al. 2024). At the same time, change in optical and electrical properties is attractive for optoelectronic devices and terahertz technology. The development of technology for creating a single-crystal InSe optical fiber was described in (Xin et al. 2024), where a polycrystalline fiber core was formed by stretching the molten InSe powder and re-crystallization of InSe induced by a CO_2 laser was used to obtain the desired fiber characteristics.

This work studies the formation of InSe amorphous thin-film samples by vacuum thermal evaporation and their optical, electrical, Raman spectra characteristics, and thermal and laser crystallization features.

Methods and materials

A quartz ampoule containing semiconductor grade (5N) starting components, taken in stoichiometric proportions, was vacuum-sealed to a residual pressure of $P = 10^{-2}$ Pa. Synthesis was performed by melting elements directly in a vacuumized quartz ampoule in a resistive heating furnace equipped with a rotation system for melt homogenization. The mixture was heated from room temperature to 660 °C at a heating rate of 1.5 °C/min. The melt was maintained for two hours at a temperature of 250 °C, which is above the melting point of selenium.

X-ray diffraction (XRD) patterns of the synthesized samples were studied using a D8 ADVANCE (Bruker) diffractometer to investigate the structure of the bulk InSe compound. Elemental analysis of the sample was performed using X-ray fluorescence (XRF) spectroscopy (M1 Mistral spectrometer).

Thermal analysis of the synthesized material was conducted using a TA Instruments Q600 SDT device, which enables simultaneous measurements of differential scanning calorimetry (DSC) and thermogravimetry (TGA). The analyses were performed in an argon atmosphere with heating and cooling rates of 10 °C/min and the maximum heating temperature of 700 °C.

 https://www.doi.org/10.33910/2687-153X-2025-6-2-93-103

The diffuse reflectance of the bulk InSe compound was determined using Cary 5000 (Agilent) spectrophotometer equipped with an integrating sphere of 150 mm in diameter with a wavelength step of 1 nm.

The formation of amorphous films of the studied chalcogenide semiconductor was ensured by the vacuum thermal evaporation method using the UVN-2M setup. The film deposition process employed a molybdenum boat as a resistive evaporator. The pressure in the chamber was 4×10^{-3} Pa, with the distance of 15.5 cm between the substrate and the evaporator and the sample weight of ~ 5 mg. The samples were coated with a 20 nm thick SiO_2 layer using the electron beam method to minimize material degradation and oxidation during subsequent heat treatment. Corning glass 1737F was used as sample substrates for laser irradiation and recording of Raman spectra, silicon substrates for determining thickness, phase and elemental composition, and oxidized silicon substrates for studying the temperature dependence of specific resistivity.

The elemental composition of the thin films was analyzed using a Tescan Amber scanning electron microscope equipped with an energy-dispersive X-ray (EDX) spectrometer. The thickness of the InSe thin films was determined using atomic force microscopy (AFM, scanning probe microscope Solver PRO", NT-MDT) in the semi-contact mode. The thickness of the SiO_2 layer was estimated using an Ellips-1881A ellipsometer. The temperature dependence of the resistivity of the thin films was measured in the range from room temperature to 300 °C. Measurements were carried out in an argon atmosphere with heating/cooling rates of 5 °C/min.

The structure of the synthesized bulk material and thin films before and after thermal or laser treatment was identified using Raman spectroscopy. The Raman spectra were measured at room temperature using a Centaur U HR spectrometer (λ = 532 nm, edge filter from 50 cm^{-1}, monochromator with a dispersion of 1.3 nm/mm and spectral resolution of at least 1 cm^{-1}). The spectrum accumulation time was 1 min, and the laser radiation power, 0.4 mW.

The irradiation of amorphous InSe films was carried out using a continuous wave Nd^{3+}:YAG laser with a wavelength of 532 nm. The laser radiation (TEM_{00} mode) was focused using a lens with a focal length of 100 mm, resulting in a spot with a diameter of about 50 μm on the film surface. The exposure time was 100 ms. The laser exposure was studied at light beam powers in the range from 10 to 330 mW. Since the crystalline phase of InSe is characterized by a higher reflection coefficient in the visible range than the amorphous one (El-Nahass et al. 2012), the results of the laser radiation on thin films were analyzed using an optical microscope (Altami MET 3T).

Results and discussions

InSe bulk samples

The X-ray fluorescence analysis of the elemental composition of the bulk InSe sample revealed a spectrum containing only the analytical peaks corresponding to selenium (Se) and indium (In). No impurities were detected above the detection limit of the device. An assessment of the elemental composition led to concentration values of $C_{wt.\%In}$ = 59.2 ± 0.8% and $C_{wt.\%Se}$ = 40.8 ± 1.1%, which are close to the expected ones.

The phase analysis of the InSe compound was performed using XRD and was followed by the Rietveld method applied in the TOPAS 4.2 software package. We established that the material crystallizes into a hexagonal structure. The refined unit cell parameters are a = 4.005 Å, b = 4.005 Å, and c = 16.400 Å. These parameters are consistent with literature data (Alieva et al. 2020).

The DSC and TGA measurements are presented in Fig. 1. The DSC curves exhibit two distinct endothermic peaks, one at 602 °C and the other at 620 °C. The melting temperature of the material, established as 602 °C, agrees with literature data (Bergeron et al. 2020). According to (Tedenac et al. 1997; Vassilev et al. 1998), the higher-temperature endothermic peak at 620 °C corresponds to the liquidus temperature of the InSe compound. After this peak, a sharp decrease in mass is observed in the TGA data, which is attributed to the evaporation of the material.

Fig. 2 shows the Raman spectrum obtained for the bulk material. Due to the crystalline nature of the material, the spectrum was decomposed into a set of peaks using the Lorentz function (Strubbe et al. 2015; Yuan, Mayanovic 2017). The positions of the peak maxima for the polycrystalline material are recorded near 111, 173, and 224 cm^{-1}, which corresponds to the vibrations of the A^1_{1g}, E^1_{2g}, and A^2_{1g} modes of InSe structural units (Wu et al. 2019; Xie et al. 2021). The signal in the region of 120–145 cm^{-1} can be attributed to a small number of chains of Se atoms between InSe clusters, which can be more significant in the amorphous state, while the signal around 245 cm^{-1} may be associated with two-phonon scattering (Weszka et al. 2000).

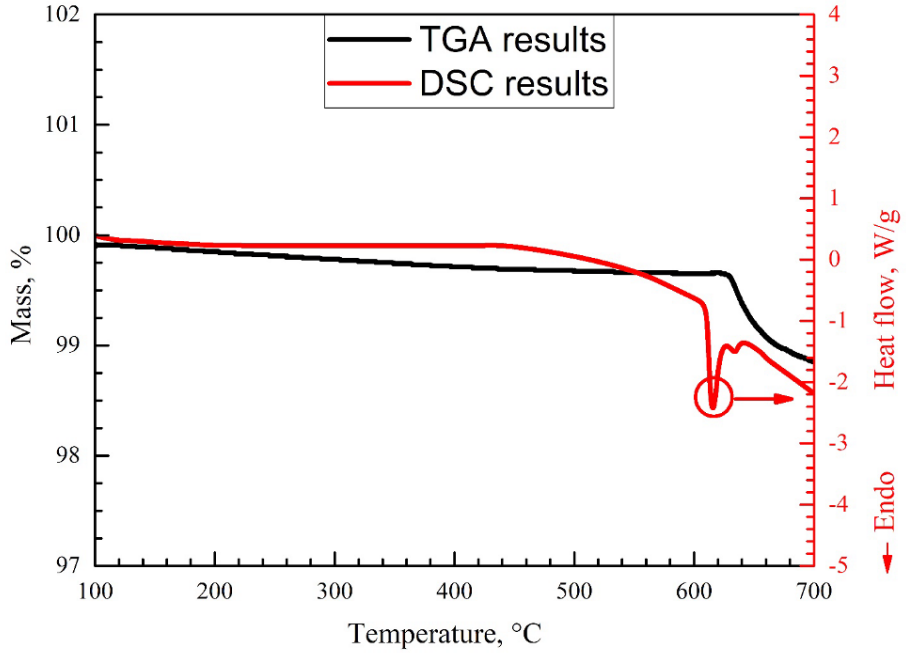

Fig. 1. DSC and TGA measurements of synthesized polycrystalline InSe

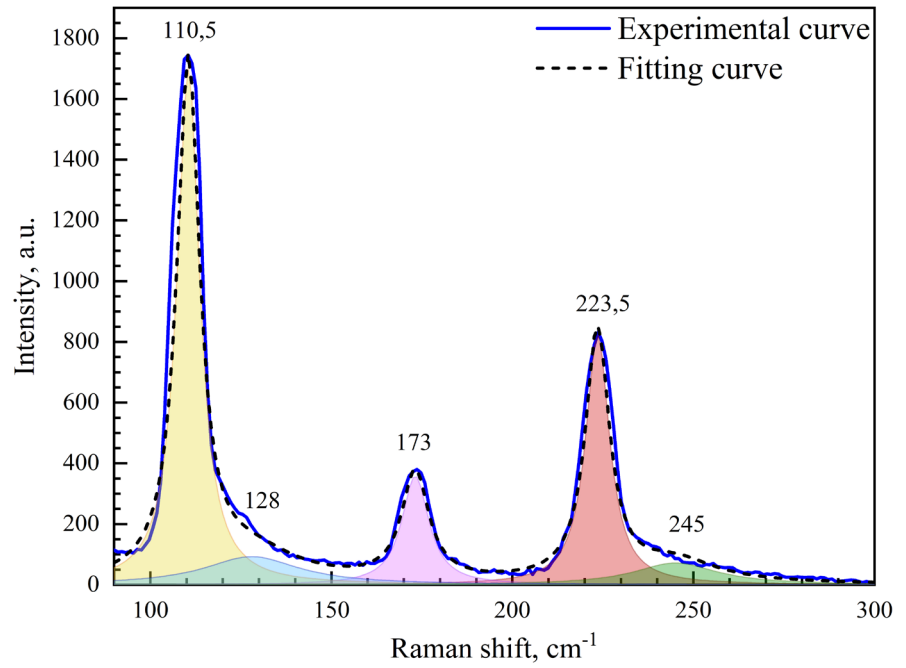

Fig. 2. Raman spectrum of bulk InSe

The results of the diffuse reflectance spectra measurements for the milled synthesized InSe are presented in Fig. 3. These data were processed using the Kubelka–Munk equation, which enabled the determination of the optical absorption edge (Kortüm et al. 1963)

$$F\left(R_d\right)=\frac{\left(1-R_d\right)^2}{2\cdot R_d}, \quad (1)$$

where R_d is diffuse reflection and $F(R_d)$ is a parameter proportional to the absorption coefficient.

 https://www.doi.org/10.33910/2687-153X-2025-6-2-93-103

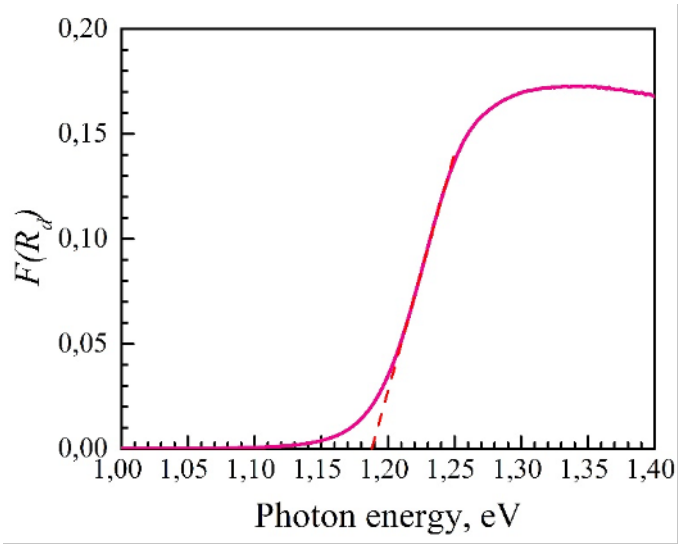

Fig. 3. Spectral dependence of the diffuse reflection of bulk InSe and estimation of the optical band gap (inset)

The optical band gap of the synthesized InSe material was determined from the intersection point of the tangent with the abscissa axis in the $F(R_d)$ energy dependence (Tarasov et al. 2023) as illustrated in Fig. 3 (inset). The obtained value of the optical band gap is 1.2 eV, which is in agreement with literature data (Olguín et al. 2003).

InSe thin-film samples

EDX microanalysis of the InSe thin films revealed spectrograms presented in Fig. 4, which clearly exhibit pronounced reflections corresponding to indium and selenium. Additionally, the spectra show peaks associated with a low carbon content. The study of areas of 200×200 mkm^2, shown in the upper images in Fig. 4, confirm the uniformity of In and Se distribution over the surface of the studied sample.

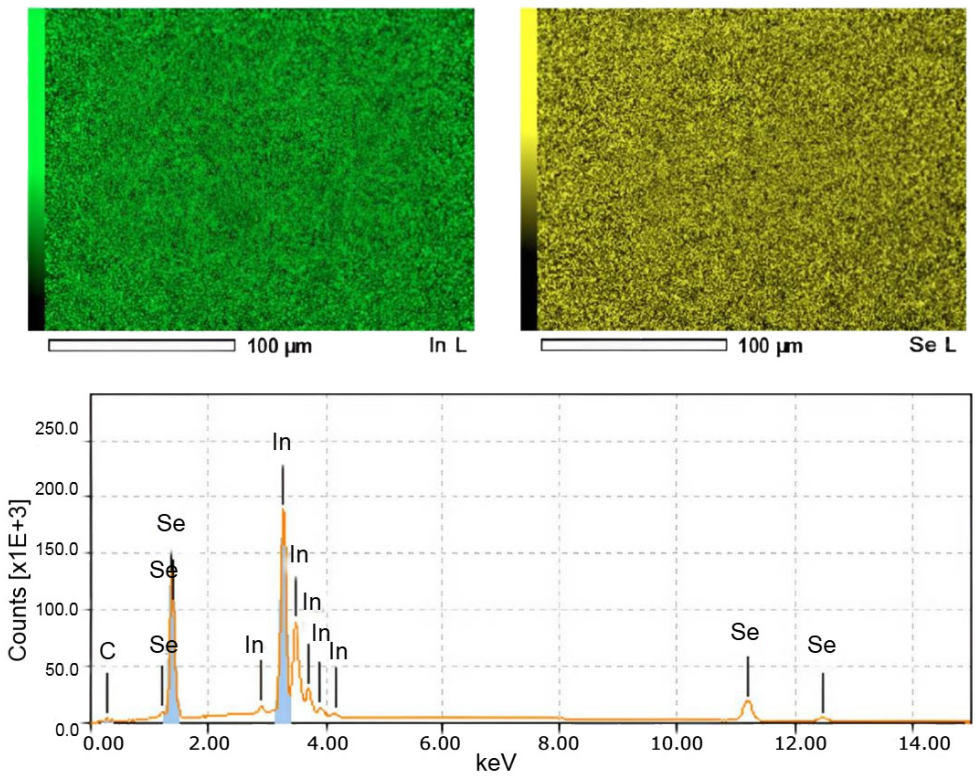

Fig. 4. EDX results of InSe thin film deposited by vacuum thermal evaporation. The upper images show the distribution of In and Se elements over the film surface, while the lower graph shows the elemental composition of the studied area

According to the atomic force microscopy measurements, the thickness of the deposited films was 16 nm with a surface roughness not above 1 nm. Ellipsometry made it possible to obtain the thickness of the protective SiO_2 layer, which was approximately 20 nm.

The temperature dependence of the resistivity of the InSe thin film is presented in Fig. 5. The sample was heated from room temperature to 300 °C. A notable feature in this dependence is a sharp decrease of resistivity from 5×10^3 to 1×10^{-1} Ohm×cm, observed in the temperature range from 210 to 235 °C. This significant drop is attributed to the crystallization of the thin film.

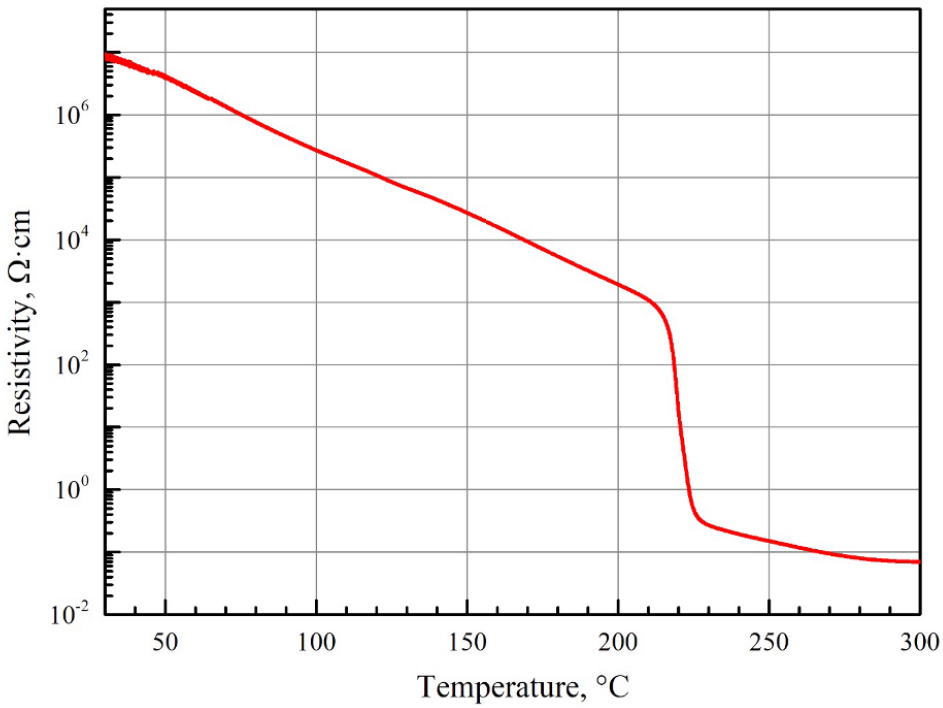

Fig. 5. Temperature dependence of the resistivity of the InSe thin film

To identify the expected structural changes, Raman spectra were measured for the as-deposited InSe film and the film annealed in an argon atmosphere for 20 minutes at 250 °C. The results are shown in Fig. 6.

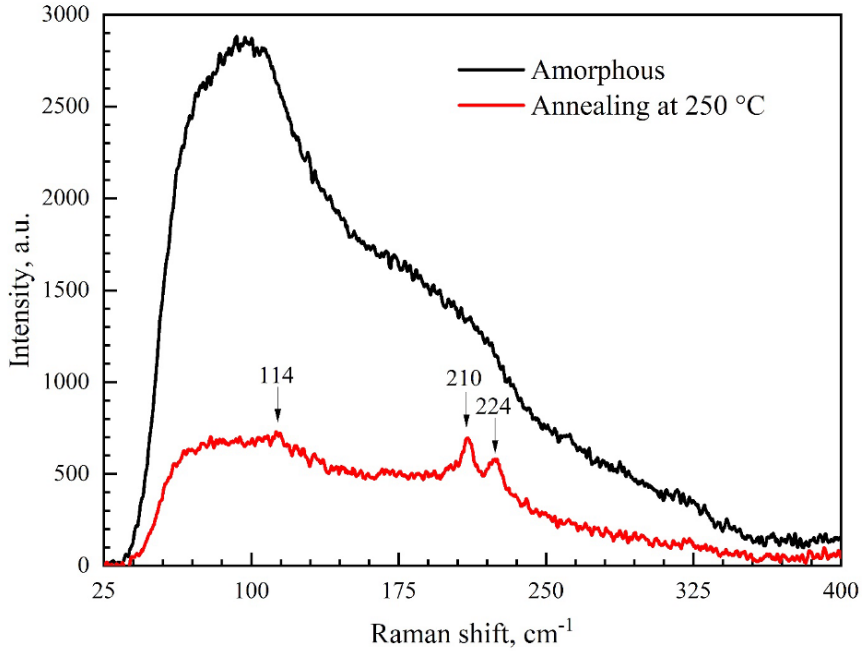

Fig. 6. Raman spectra for the as-deposited amorphous film and the film annealed at 250 °C

https://www.doi.org/10.33910/2687-153X-2025-6-2-93-103

The Raman spectroscopy showed that the shape of the spectra of the InSe films thermally treated at 250 °C and coated with a protective SiO_2 layer differs significantly from the spectra obtained from the initial amorphous films. As a result of the thermal treatment, peaks near 114, 210, and 224 cm^{-1} appear in the spectrum; the last two peaks are quite narrow. Comparison of the positions of these peaks with the peaks in the spectrum obtained from the polycrystalline bulk material (Fig. 2) showed that these peaks correspond to the A^1_{1g} and A^2_{1g} (114 and 224 cm^{-1}) vibrational modes of InSe structural units, characteristic of the crystalline state (Wu et al. 2019; Xie et al. 2021). Additionally, a narrow peak at about 210 cm^{-1}, which appears relative to the spectrum of the polycrystalline bulk material, can be attributed to E'(LO) vibrations, which appear along with the A^1_{1g} and A^2_{1g} peaks for polycrystalline InSe in the form of hexagonal sheets (Choi et al. 2003). A similar peak was observed for hexagonal InSe film synthesized on a graphite (HOPG) substrate (Voigt et al. 2024a).

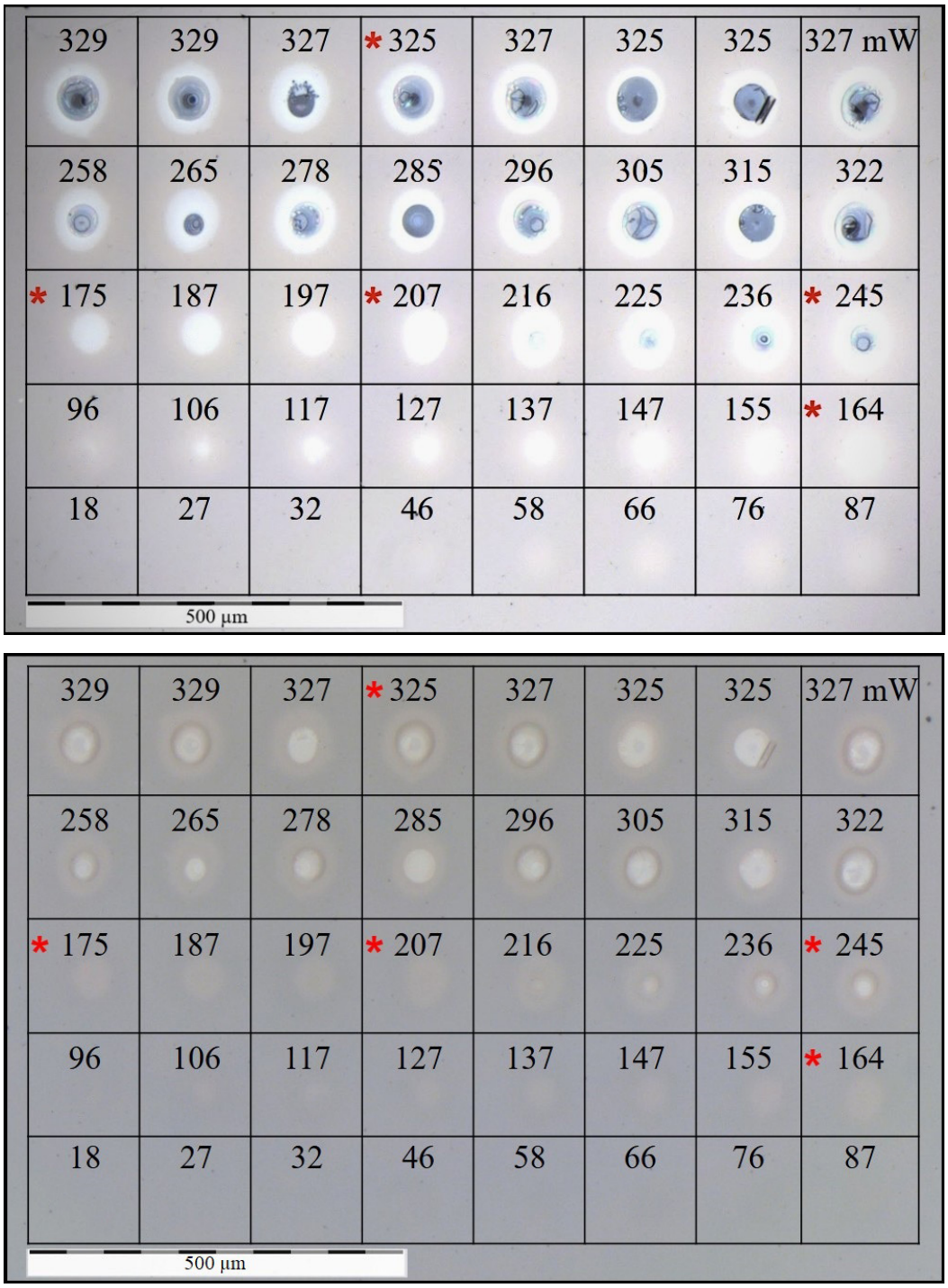

Fig. 7. Optical microscope images of a laser-irradiated InSe thin film in reflected (a) and transmitted (b) backlight modes (the regions where Raman spectra were measured are marked with the * symbol)

The optical microscopy images of the InSe films illuminated by a cw-laser were obtained in reflected (Fig. 7a) and transmitted (Fig. 7b) backlight regimes. It is evident from the figures that all illuminated areas can be divided into three groups. The first group consists of areas resulting from irradiation with laser powers ranging from 18 to 96 mW. The reflectivity of the film remains unchanged or undergoes only minor changes. An analysis of the Raman spectra reveals that in this case laser exposure does not induce any phase transformation of InSe. Corresponding Raman spectra are identical to those obtained from the original as-deposited (non-irradiated) film, as illustrated by the black and green curves in Fig. 8.

The second group comprises areas formed as a result of laser exposure with powers from 96 to 207 mW. The reflectivity of these areas is significantly higher than that of the as-deposited amorphous film. The Raman spectra exhibit peaks with maxima near 112, 210, and 225 cm^{-1}, which are characteristic of a crystalline phase of InSe. As the radiation energy goes up from 164 to 207 mW, the intensity of these peaks also increases, indicating a rise in the degree of crystallinity of the modified InSe areas. This suggests that higher laser powers enhance the crystallization process.

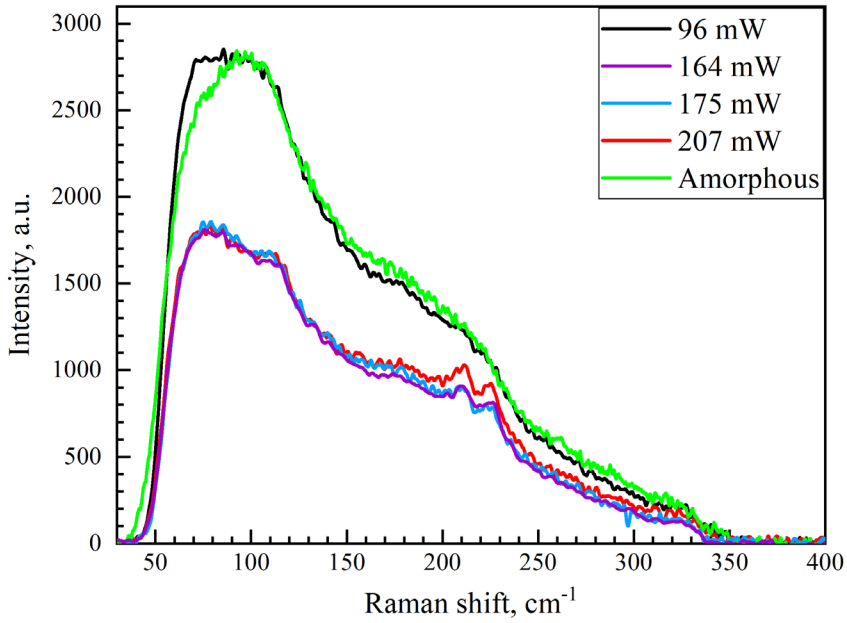

Fig. 8. Raman spectra of the InSe thin film coated with SiO_2 in areas after laser exposure with a different power

The third group comprises areas resulting from irradiation with a laser power exceeding 207 mW. As follows from Fig. 7, the central part of the irradiated area, where the laser radiation energy is maximal due to Gaussian intensity distribution, shows material ablation or degradation. That is clearly confirmed by the fact that the irradiated areas of the film (at powers above 216 mW) become bright in the optical microscope transmission mode (Fig. 7b), i. e. the transparency of the samples increases with the destruction of InSe, tending to the transmission of the glass substrate. The higher the radiation energy, the larger the ablation or degradation area. At the periphery of the irradiation area, corresponding to the tails of the Gaussian radiation intensity distribution, regions with increased reflectivity are observed. These regions are similar to those in group 2 but display a lower intensity in both the specific peaks and the overall Raman spectrum compared to areas modified by laser powers between 117 and 207 mW. This reduction in intensity is attributed to the partial evaporation of the material due to the small thickness of the InSe film and the SiO_2 protective film. This is also confirmed by the fact that the ablation threshold of SiO_2 is obviously not exceeded by the laser action used in present work (Mangersnes et al. 2010; Rublack et al. 2011).

Conclusions

Studies of InSe bulk samples showed that the synthesized material is close to the declared stoichiometric composition, with the melting point of 602 °C and the optical band gap of 1.2 eV. The use of vacuum thermal evaporation enabled the production of thin amorphous films, opening up opportunities

 https://www.doi.org/10.33910/2687-153X-2025-6-2-93-103

for studying phase transformations in InSe upon heating or as a result of laser irradiation. Thin-film InSe samples were passivated with a SiO_2 film for protection against oxidation and mechanical damage.

The temperature dependence of film resistivity showed that phase transition from the amorphous to the crystalline state is in the range from 210 to 235 °C. Raman studies performed for the film annealed at 250 °C confirmed its crystallization by the presence of characteristic peaks. Laser irradiation of thin films was carried out in the power range from 10 to 330 mW. At low optical powers (up to 96 mW), film crystallization is practically not observed, either with an optical microscope or by Raman spectroscopy. At powers from 96 to 207 mW, film crystallization occurs partially, and with an increasing power, the intensity of the Raman scattering peaks corresponding to the crystalline phase rises. Above 207 mW, film ablation begins, and InSe destruction is observed within the irradiated areas. Thus, threshold values of temperatures and laser powers necessary for the crystallization of amorphous InSe thin films formed by vacuum thermal evaporation were determined.

Conflict of Interest

The authors declare that there is no conflict of interest, either existing or potential.

Author Contributions

Optical and electrophysical measurements, writing — original draft preparation: M. E. Fedyanina; AFM and Raman measurements: V. B. Pestova, A. V. Romashkin; synthesis and deposition of films: D. V. Pepelyaev; laser irradiation of thin films: Ya. S. Lebedeva, M. P. Smayev; DSC measurements: A. V. Babich, supervision: S. A. Kozyukhin, S. I. Nesterov.

References

Alieva, I. I., Mamedova, N. A., Sadygov, F. M. et al. (2020) Investigation of chemical interactions in the Sb_2Te_3-InSe system and properties of the obtained phases. *Russian Journal of Inorganic Chemistry*, 65 (10), 1585–1590. http://dx.doi.org/10.1134/S0036023620100010 (In English)

Bandurin, D. A., Tyurnina, A. V., Yu, G. L. et al. (2017) High electron mobility, quantum Hall effect and anomalous optical response in atomically thin InSe. *Nature Nanotech*, 12, 223–227. https://doi.org/10.1038/nnano.2016.242 (In English)

Bergeron, H., Guiney, L. M., Beck, M. E. et al. (2020) Large-area optoelectronic-grade InSe thin films via controlled phase evolution. *Applied Physics Reviews*, 7, article 041402. https://doi.org/10.1063/5.0023080 (In English)

Chang, H-C., Tu, C-L., Lin, K. et al. (2018) Synthesis of Large-Area InSe Monolayers by Chemical Vapor Deposition. *Small*, 14 (39), article 1802351. https://doi.org/10.1002/smll.201802351 (In English)

Choi, I. H., Yu, P. Y. (2003) Properties of phase-pure InSe films prepared by metalorganic chemical vapor deposition with a single-source precursor. *Journal of Applied Physics*, 93 (8), 4673–4677. https://doi.org/10.1063/1.1561584 (In English)

Dai, M., Chen, H., Feng, R. et al. (2018) A dual-band multilayer InSe self-powered photodetector with high performance induced by surface Plasmon resonance and asymmetric Schottky junction. *ACS Nano*, 12 (8), 8739–8747. https://doi.org/10.1021/acsnano.8b04931 (In English)

Darwish, A. A. A., El-Nahass, M. M., Bahlol, M. H. (2013) Structural and electrical studies on nanostructured InSe thin films. *Applied Surface Science*, 276, 210–216. https://doi.org/10.1016/j.apsusc.2013.03.068 (In English)

El-Nahass, M. M., Saleh, A-B. A., Darwish, A. A. A. Bahlol, M. H. (2012) Optical properties of nanostructured InSe thin films. *Optics Communications*, 285 (6), 1221–1224. https://doi.org/10.1016/j.optcom.2011.11.031 (In English)

Emery, J. Y., Brahim-Otsmane, L., Jouanne, M. et al. (1989) Growth conditions of In_xSe_y films by molecular beam deposition. *Materials Science and Engineering: B*, 3 (1-2), 13–17. https://doi.org/10.1016/0921-5107(89)90172-4 (In English)

Feng, W., Wu, J., Li, X. et al. (2015) Ultrahigh photo-responsivity and detectivity in multilayer InSe nanosheets phototransistors with broadband response. *Journal of Materials Chemistry C*, 3, 7022–7028. https://doi.org/10.1039/C5TC01208B (In English)

Gopal, S., Viswanathan, C., Thamilselvan, M. et al. (2004) Conduction studies on electrodeposited indium selenide thin films. *Ionics*, 10, 300–303. https://doi.org/10.1007/BF02382835 (In English)

Khusayfan, N. M., Qasrawi, A. F., Khanfar, H. K., Alharbi, S. R. (2024) Fast crystallization of InSe thin films via pulsed laser welding technique and effect of crystallinity on the optical and dielectric properties. *Physica Scripta*, 99 (2), article 025988. https://doi.org/10.1088/1402-4896/ad2040 (In English)

Kobbi, B., Kesri, N. (2004) Physico-chemical and electrical properties of InSe films. *Vacuum*, 75 (2), 177–182. https://doi.org/10.1016/j.vacuum.2004.02.003 (In English)

Kortüm, G., Braun, W. Herzog, G. (1963) Principles and techniques of diffuse-reflectance spectroscopy. *Angewandte Chemie*, 2 (7), 333–341. https://doi.org/10.1002/anie.196303331 (In English)

Kovalyuk, Z. D., Katerynchuk, V. M., Mintyanskii, I. V. et al. (2005). γ-Radiation influence on the photoelectrical properties of oxide–p-InSe heterostructure. *Materials Science and Engineering: B*, 118 (1-3), 147–149. https://doi.org/10.1016/j.mseb.2004.12.024

Lebedeva, Y. S., Smayev, M. P., Budagovsky, I. A. et al. (2023) Photoinduced Crystallization of Sb_2Se_3 and $Ge_2Sb_2Te_5$ Chalcogenide Films. *Journal of Surface Investigation*, 17, 339–348. https://doi.org/10.1134/S1027451023070297 (In English)

Mangersnes, K., Foss, S. E., Thogersen, A. (2010) Damage free laser ablation of SiO_2 for local contact opening on silicon solar cells using an a-Si:H buffer layer. *Journal of Applied Physics,* 107 (4), article 043518. http://dx.doi.org/10.1063/1.3309382 (In English)

Mustafa, F. I., Gupta, S., Goyal, N., Tripathi, S. K. (2010) Effect of indium concentration on the electrical properties of InSe alloy. *Physica B: Condensed Matter*, 405 (19), 4087–4091. https://doi.org/10.1016/j.physb.2010.06.006 (In English)

Olguín, D., Cantarero, A., Ulrich, C., Syassen, K. (2003) Effect of pressure on structural properties and energy band gaps of γ-InSe. *Physica Status Solidi (b)*, 235 (2), 456–463. https://doi.org/10.1002/pssb.200301602 (In English)

Park, J-H., Afzaal, M., Helliwell, M. et al. (2003) Chemical vapor deposition of indium selenide and gallium selenide thin films from mixed Alkyl/Dialkylselenophosphorylamides. *Chemistry of Materials*, 15 (22), 4205–4210. https://doi.org/10.1021/cm0310420 (In English)

Prikryl, J., Mistrik, J., Krbal, M. (2022) Optical properties of as-deposited, annealed and laser-treated $Ge_2Sb_2Te_5$ thin films. *Optical Materials Express*, 12, 2927–2937. https://doi.org/10.1364/OME.462278 (In English)

Rani, R., Dimple, D., Jena, N. et al. (2017) Controlled formation of nanostructures on MoS_2 layers by focused laser irradiation. *Applied Physics Letters*, 110, article 083101. https://doi.org/10.1063/1.4976692 (In English)

Rublack, T., Hartnauer, S., Kappe, P. et al. (2011) Selective ablation of thin SiO_2 layers on silicon substrates by femto- and picosecond laser pulses. *Applied Physics A*, 103, 43–50. http://dx.doi.org/10.1007/s00339-011-6352-x (In English)

Rybin, M. V., Sinelnik, A. D., Tajik, M. et al. (2021) Optically reconfigurable spherical Ge-Sb-Te nanoparticles with reversible switching. *Laser & Photonics Reviews*, 16 (2), article 2100253. https://doi.org/10.1002/lpor.202100253 (In English)

Smayev, M. P., Smirnov, P. A., Budagovsky, I. A. et al. (2024) Cylindrical laser beams for a-$Ge_2Sb_2Te_5$ thin film modification. *Journal of Non-Crystalline Solids*, 633, article 122952. https://doi.org/10.1016/j.jnoncrysol.2024.122952 (In English)

Song, Ch., Huang, Sh., Wang, Ch. et al. (2020) The optical properties of few-layer InSe. *Journal of Applied Physics*, 128, article 060901. https://doi.org/10.1063/5.0018480 (In English)

Stepanov, R. S. (2024) Uniaxial pressure modulation of two-dimensional materials: Insights into the structure and electronic properties of $MoTe_2$ and Sb_2Te_3. *Physics of Complex Systems*, 5, 30–38. https://doi.org/10.33910/2687-153X-2024-5-1-30-38 (In English)

Strubbe, D. A., Johlin, E. C., Kirkpatrick, T. R. et al. (2015) Stress effects on the Raman spectrum of an amorphous material: Theory and experiment on a -Si:H. *Physical Review B*, 92, article 241202. https://doi.org/10.1103/PhysRevB.92.241202 (In English)

Tarasov, A., Dubkov, S., Vigdrovich, E. et al. (2023) Photocatalytic reduction of CO_2 over TiO_2 nanowires catalyst. *MATEC Web of Confere*nces, 376, article 01011. https://doi.org/10.1051/matecconf/202337601011 (In English)

Tedenac, P. J.-C., Vassilev, D. G. P., Daouchi, B. et al. (1997) Low-temperature Region of the In–Se System. *Crystal Research and Technology*, 32 (4), 605–616. https://doi.org/10.1002/crat.2170320417 (In English)

Tran-Khac, B-C., White, R., DelRio, F. Chung, K-H. (2019) Layer-by-layer thinning of MoS_2 via laser irradiation. *Nanotechnology*, 30, article 275302. http://dx.doi.org/10.1088/1361-6528/ab11ad (In English)

Vassilev, G. P., Daouchi, B., Record, M., Tedenac, J. (1998) Thermodynamic studies of the In–Se system. *Journal of Alloys and Compounds*, 269, 107–115. https://doi.org/10.1016/S0925-8388(98)00007-3 (In English)

Voigt, C. A., Reingold, M., Dube, A. et al. (2024a) Molecular beam epitaxy synthesis of In_2Se_3 films. *Journal of Vacuum Science & Technology A*, 42 (3), article 032707. https://doi.org/10.1116/6.0003508 (In English)

Voigt, C. A., Tian, M., Peacock, R. et al. (2024b) Quantitative Raman and x-ray photoelectron spectroscopy of mixed-phase indium selenide films. *Journal of Applied Physics*, 135 (21), article 215301. http://dx.doi.org/10.1063/5.0202596 (In English)

Wang, Y., Gao, J., Wei, B. et al. (2020) Reduction of the ambient effect in multilayer InSe transistors and a strategy toward stable 2D-based optoelectronic application. *Nanoscale*, 12, 18356–18362. https://doi.org/10.1039/D0NR04120C (In English)

Weszka, J., Daniel, P., Burian, A. M. (2000) Raman Spectra of $In_{0.30}Se_{0.70}$ Amorphous Films. *Acta Physica Polonica A*, 98 (5), 619–623. (In English)

Wu, M., Xie, Q., Wu, Y. et al. (2019) Crystal structure and optical performance in bulk γ-InSe single crystals. *AIP Advances*, 9 (2), article 025013. https://doi.org/10.1063/1.5086492 (In English)

Xie, Q., Hu, C., Xu, L. et al. (2021) Stability studies of few-layer InSe nanosheets by Raman spectroscopy. *Solid State Communications*, 336, article 114417. https://doi.org/10.1016/j.ssc.2021.114417 (In English)

Xin, L., He, H., Wang, X. et al. (2024) Single-crystalline indium selenide fibers by laser-induced recrystallization and their tunable whispering-gallery-mode lasing by pressure-modulating. *Journal of the American Ceramic Society*, 107 (9), 5801–5809. https://doi.org/10.1111/jace.19916 (In English)

Yuan, X., Mayanovic, R. A. (2017) An empirical study on Raman peak fitting and its application to Raman quantitative research. *Applied Spectroscopy*, 71 (10), 2325–2338. http://dx.doi.org/10.1177/0003702817721527 (In English)

Zhao, O., Frisenda, R., Wang, T., Castellanos-Gomez, A. (2019) InSe: A two-dimensional semiconductor with superior flexibility. *Nanoscale*, 11, 9845–9850. https://doi.org/10.1039/C9NR02172H (In English)